SCIENTIFIC REPORTS
nature research

OPEN

Monodisperse thiourea functionalized graphene oxide-based PtRu nanocatalysts for alcohol oxidation

Esra Kuyuldar[1], Su Selda Polat[1], Hakan Burhan[1], Sibel Demiroglu Mustafov[1], Aysegul Iyidogan[2] & Fatih Sen[1] ✉

Addressed herein, thiourea functionalized graphene oxide-based PtRu nanocatalysts (PtRu@T/GO) has been synthesized and characterized by several techniques and performed for methanol oxidation reactions as novel catalysts. In this study, graphene oxide (GO) was functionalized with thiourea (T/GO) in order to obtain monothiol functionalized graphene and increase the stability and activity of the nanocatalysts. Raman spectroscopy, X-ray photoelectron spectroscopy (XPS), X-ray diffraction (XRD), TEM (transmission electron microscopy) and high-resolution transmission electron microscopy (HR-TEM) were used for characterization of the prepared nanocatalysts. The results obtained from these techniques showed that the prepared nanocatalysts were in a highly crystalline form, well dispersed on T/GO, very small in size and colloidally stable. The average size of the synthesized nanocatalysts determined by TEM analysis was found to be 3.86 ± 0.59 nm. With HR-TEM analysis, the atomic lattice fringes of the nanocatalysts were calculated to be 0.23 nm. After the full characterization of the prepared nanocatalysts, they were tried for the methanol oxidation reaction (MOR) and it was observed that 97.3% of the initial performance was maintained even after 1000 cycles while exhibiting great catalytic activity and stability with the help of T/GO. Thus, the arranged nanocatalysts displayed great heterogeneous catalyst characteristics for the methanol oxidation response.

The direct methanol fuel cells (DMFCs) have superior properties among reliable and long-lasting portable power sources used in devices such as mobile phones, computers, etc. Even though there are substantial improvements in DMFC systems over the last decade, more effort is needed to commercialize DMFCs by producing durable, low cost and lower size devices. Up to now, the many present nanocatalysts have been developed as electrocatalysts for DMFCs, but it is really important to obtain the optimum supporting agents that enhance the interaction and the catalytic activity between the support material and the metal catalyst[1–6]. As a catalyst support material, carbon derivatives have been commonly used[7–12]. The results of intensive studies on carbon-containing materials revealed some significant information about the catalytic activity and supporting agents[13–15]. The synthesis of nanomaterials is very important in the use of DMFCs. Specifically, nanocatalysts containing carbon-based materials[16–21] such as carbon nanohorns, carbon nanofibers, carbon nanotubes, and carbon nano-coils have attracted attention. When compared to traditional materials, carbon-based materials have unique advantages[22–26] such as high corrosion resistance, better electrical conductivity, and less catalyst poisoning[27–29]. The electrocatalyst based on these carbon-based materials used in fuel cells must have some desirable features such as composed of reactants facilitating reactions, controllable suitable particle size, etc.

Various methods have been used to prepare surface-functionalized carbon-based nano-catalysts[22,23,30–32]. Therefore, various catalysts[33–42] such as Pt and Ru based have been used as electrocatalysts (PtRuWC, PtRuIr, PtRuCo, PtRuP, PtRuSnW, and PtRuRhNi). Among those, PtRu based catalysts have been extensively used for the catalytic reaction in the anode of DMFC due to their long life and the suitable surface. However, there are various problems to be overcome for these types of catalysts. For instance, insufficient durability, inactivity, crossover problem and dissolution[38,43–50] are essential problems related to carbon-based PtRu catalysts. In order

[1]Sen Research Group, Department of Biochemistry, Faculty of Arts and Science, Dumlupınar University, Evliya Çelebi Campus, 43100, Kütahya, Turkey. [2]Department of Chemistry, Faculty of Science and Arts, Gaziantep University, Gaziantep, Turkey. ✉e-mail: fatihsen1980@gmail.com

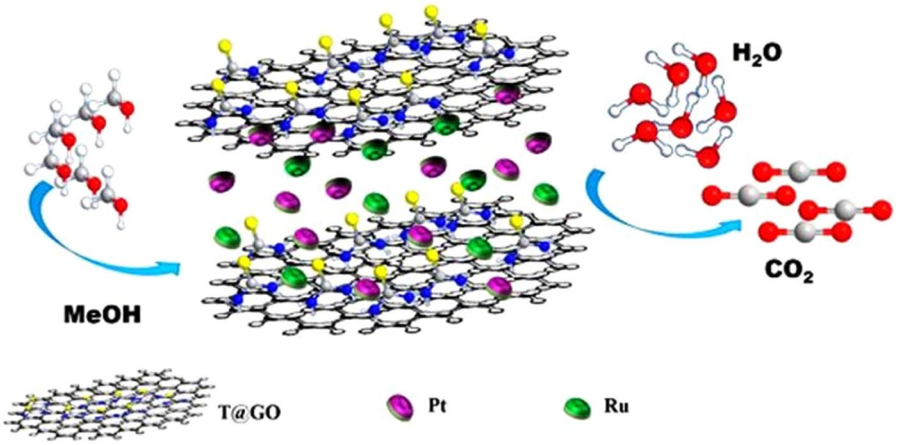

Figure 1. Schematic illustration of PtRu@T/GO nanocatalysts for methanol oxidation.

to solve those types of problems, some studies have been performed with the help of the functionalization of carbon-based materials, etc.[51–56]. Consequently, graphene oxide was functionalized mainly with different functional groups containing heteroatoms for improving the physical and chemical properties of graphite[38,47–51,57–61].

In this study, we have investigated the thiourea based graphene oxide (T/GO) as a potential supporting and stabilizing agent. Functionalization of graphene oxide with thiourea (T) ensures diversified potentialities to enhance the usage of graphene and increase the chemical conversion to graphene. This eliminates its poor solubility and difficult processability in both water and organic solvents make it one of the ideal materials for MOR. Here, we report for the first time that we used the thiourea graphene oxide-supported PtRu nanocatalysts (PtRu@T/GO) as the anode catalyst in DMFCs and the activity of the catalyst was enhanced due to acquiring high active sites, solubility and functionalization. Schematic illustration of PtRu@T/GO nanocatalysts for methanol oxidation was shown in Fig. 1.

Experimental

The procedure of preparation PtRu@T/GO nanocatalysts. To obtaining graphene oxide (GO) nanosheets from graphite, the modified Hummers' method was carried out as shown in supporting information in detail[62–64]. Moreover, then, 50 mg of obtained GO nanosheets were dispersed in a round-bottom flask contained 10 mL THF and 1 mg/mL thiourea (T). This mixture then respectively stirred for 1 hour and ultrasonicated for another 1 hour at room temperature. The prepared solution was filtered to obtain the dark brown material apart from the solution. The dark brown graphene oxide slurry washed with EtOH to get the T/GO nanosheets neatly and then it was dried at 50 °C in a vacuum oven overnight. Under sonication, 25 mg of $PtCl_4$, 25 mg of $RuCl_3$ and 50 mg of T/GO were mixed thoroughly in deionized water. The mixing protocol was continued at 55 °C for 12 hours. In the next step, 100 µL of DMAB solution was added dropwise with stirring over 5-minute intervals. After all the processes, washing with deionized water was carried out. Finally, the PtRu@T/GO nanocatalysts was left to dry in the vacuum oven.

Preparation of nanocatalysts sample was performed with a solution containing 0.5 mg. mL^{-1} ethanol and copper grid (carbon covered 400 mesh), resulting mixture were evaporated. Samples were morphologically examined by taking TEM images with a JEOL 200 kV instrument. The removing excess mixture was done by using adsorbent paper, and the resulting solid sample was dried at 298 K. To get an overall analysis of PtRu@T/GO nanocatalysts almost 300 particles were investigated. XPS analysis was utilized to examine the oxidation state of the metals in the nanocatalysts as well by Specs spectrometer (1253.6 eV, 10 mA). XPS analysis was performed with Gaussian function and C 1 s line at 284.6 eV taken as reference points. XRD analysis was executed to represent the composition of PtRu@T/GO nanocatalysts by Rigaku diffractometer, X-ray generator with Cu K radiation at 40 kV, 40 mA.

The activities of electrochemical nanocatalysts. After full characterization of the prepared nanocatalysts, the catalytic activities of the electrochemical catalyst were performed by a chronoamperometry (CA) (Gamry, Reference 3000) and cyclic voltammetry (CV). The three-electrode system consists of a working electrode, a counter electrode, and a reference electrode. These were a glass carbon electrode (GCE) covered with thin the catalyst, Ag/AgCl, and Pt wire, respectively. An electrolyte containing potassium hydroxide (0.5 M), methanol (0.5 M) and saturated nitrogen gas at room temperature was used to perform CA and CV analysis. In the beginning, the samples were activated in a nitrogen-saturated potassium hydroxide (0.5 M), a voltage in a range of -0.9 + 0.2 V, by CV at a rate of 50 mV/s.

Results and discussion

Characterization of the PtRu@T/GO nanocatalysts. Various analytical methods like HR-TEM, TEM, XPS, Raman spectroscopy, and XRD analyses were carried out for illuminating surface properties and morphology, chemical, and physical structure of the current nanocatalysts. For instance, the TEM analysis images are shown in Figs. 2a and S1 and they revealed that the composition of the PtRu@T/GO nanocatalyst was homogeneous, and the mean diameter of the particles was found to be 3.86 ± 0.59 nm (Fig. 2b). Also, these findings

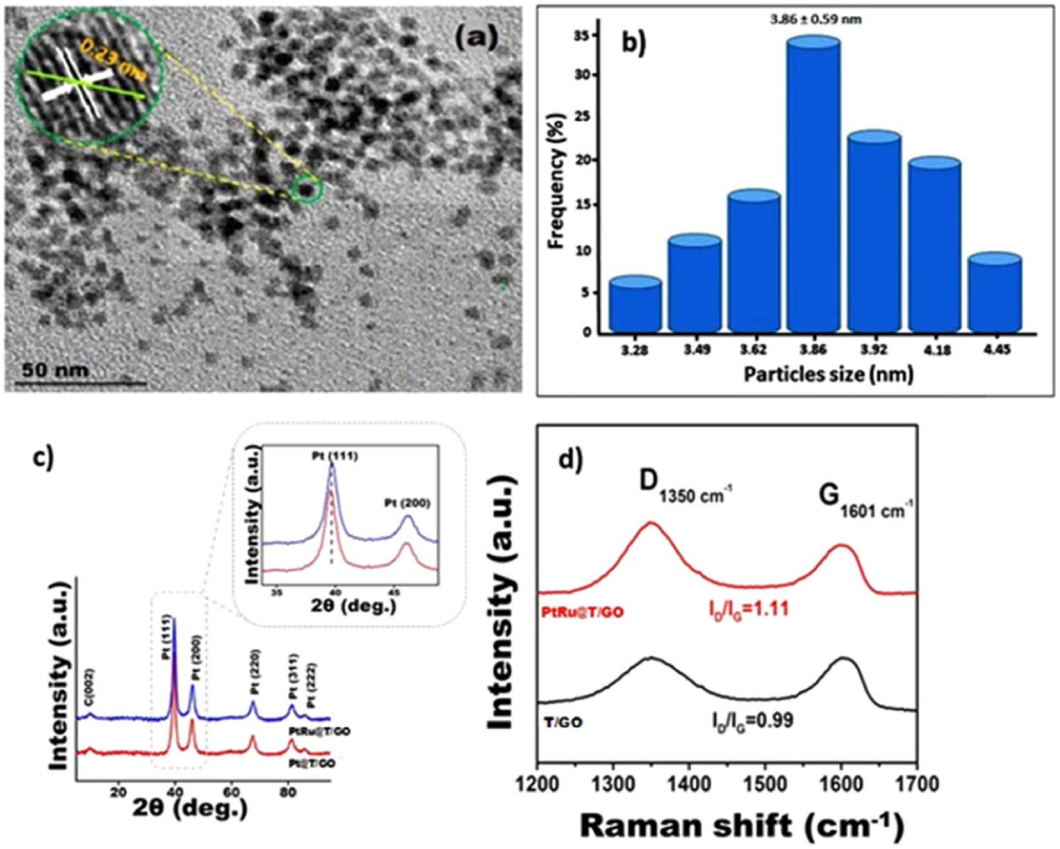

Figure 2. (**a**) TEM image of as-prepared PtRu@T/GO nanocatalysts indicating excellent catalyst morphology and (**b**) histogram, (**c**) X-ray diffraction pattern of as-prepared Pt@T/GO and PtRu@T/GO nanocatalysts. (**d**) Raman analysis of prepared materials.

according to TEM analysis during the formation of PtRu@T/GO nanocatalysts showed that no agglomeration was detected, and obtained nanocatalysts were spherical. HR-TEM analysis also indicated that the atomic lattice fringe of particles was calculated as 0.23 nm which is consistent with the data in the literature[65–69]. Further, XRD analysis was used to examine the crystal structures of the bimetallic PtRu@T/GO nanocatalysts synthesized homogeneously, and the crystal structure was compared with the crystal structure of Pt and Ru. As shown in Fig. 2c, XRD patterns of Pt@T/GO and PtRu@T/GO were examined in order to see the crystalline structure of the catalysts. As seen in the model, monodisperse PtRu nanocatalysts were found to be in the face-centered cubic (fcc) structure in the XRD model, and in this structure, five characteristic peaks are corresponding to the (111), (200), (220), (311) and (222) planes respectively for the PtRu nanocatalysts in the bimetallic structure. Besides, a peak at 12.5° is defined as T/GO, and according to data in Fig. 2b, a slight shift of 2θ values of bimetallic PtRu@T/GO nanocatalysts compared to the monometallic ones shows the alloy formation of prepared nanocatalysts.

The Scherrer Eq. (1) was utilized for calculating the average size of PtRu@T/GO nanocatalysts, and it is determined as 3.86 nm[70–72] which is consistent with TEM analysis.

$$d(\text{Å}) = \frac{k\lambda}{\beta cos\theta} \tag{1}$$

where k is a coefficient (0.9), β = a half maximum diffraction peak, θ = the angle at the position of peak maximum (rad) λ = X-ray wavelength (1.54 Å). Platinum diffraction peak (111) was used to calculate the lattice parameter values as 3.92 Å.

Raman spectroscopy was also used in order to determine the ratio of D and G bands of prepared materials as shown in Fig. 2d. The defects on the graphene assess the ratio of peak intensities for the D and G bands (ID/IG). This ratio is 0.99, and 1.11 for T/GO, and PtRu@T/GO nanocatalysts, respectively. The slightly higher degree of defects (D/G ratio) on PtRu@T/GO nanocatalysts compared to the T/GO can be explained by the functionalization of T/GO. Moreover, electronic properties, elemental structure and chemical oxidation of the metals in the PtRu@T/GO were detected by XPS analysis. In XPS analysis, ruthenium 3p and platinum 4f orbital regions were investigated; therefore, the XPS peaks were fitted to the Gaussian method and calculated with the help of the integration area of each peak. C 1 s peak at 284.6 eV was taken as a reference[73–77] for the accuracy of binding energies according to the XPS spectrum data. Experimental binding energies (Fig. 3) of ruthenium and platinum were compared to the binding energies exist in the literature. The obtained experimental binding energies for

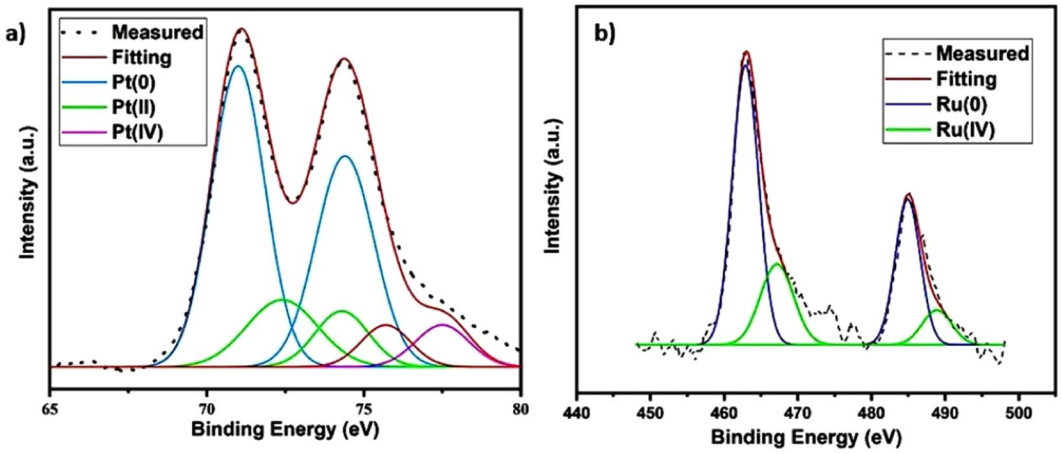

Figure 3. (**a**) 2D X-ray photoelectron spectra of Pt 4f and (**b**) 2D of X-ray photoelectron spectra of Ru 3p in PtRu@T/GO nanocatalysts.

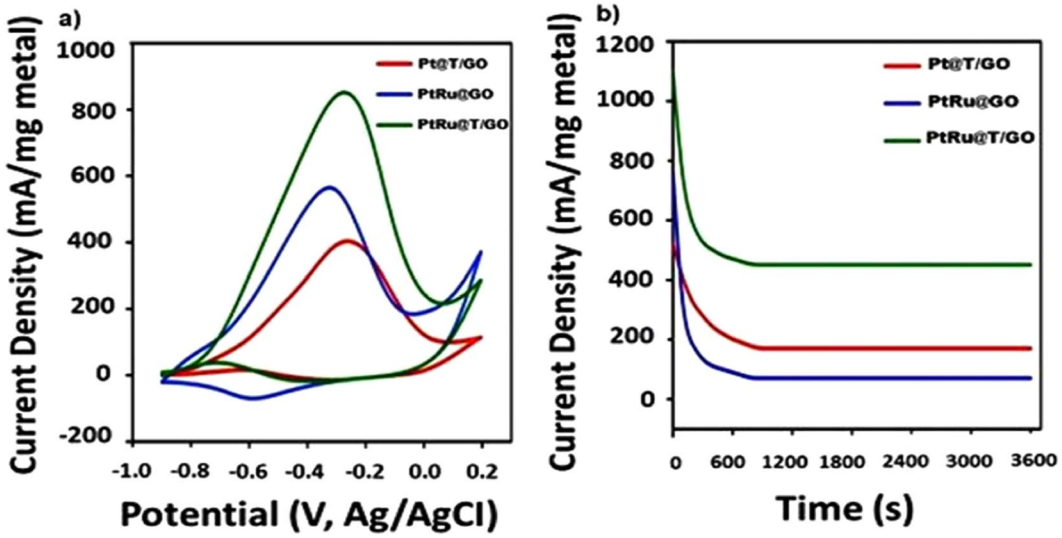

Figure 4. (**a**) Cyclic voltammograms of PtRu@T/GO and Pt@T/GO, PtRu@GO nanocatalysts in nitrogen saturated solution of 0.5 M KOH containing 0.5 M CH_3OH (Scan rate = 50 mV s^{-1}). (**b**) Chronoamperometric curves of PtRu@T/GO and Pt/T/GO, PtRu@GO in 0.5 M KOH nitrogen saturated solution containing 0.5 M CH_3OH at 0.5 V.

ruthenium and platinum are observed in 462.3 eV, and 70.2 eV, respectively. When the experimental data compared to the data exist in the literature, XPS analysis demonstrates that the surface of PtRu@T/GO has covered mostly with metals and unoxidized species. The presence of a small energy change for ruthenium at $3p_{3/2}$ indicates the formation of PtRu@T/GO nanocatalysts. Moreover, it can be stated from the experimental data in Fig. 3 that the composition of the nanocatalysts is mostly metallic due to the species of platinum (0) and ruthenium (0). Besides, there are some other peaks related to the oxidized species such as Pt (II) and Ru (IV) ions due to oxidation, as seen in Fig. 3. The peak region of platinum is greater than ruthenium since the higher sensitiveness of Pt 4f compared to the ones of Ru 3p. O 1 s XPS spectrum of PtRu@T/GO nanocatalysts (Fig. S2) displays that C-O and C=O bonds become mostly prominent while the other oxygen groups have decreased to minimum amounts as given in supporting information in detail.

Electrochemical performance of PtRu@T/GO nanocatalysts. After full characterization of the PtRu@T/GO nanocatalysts, the electrocatalytic activity of these catalysts towards methanol oxidation was studied in Fig. 4a (0.5 M KOH solution saturated with N_2 gas in 0.5 M CH_3OH). As can be observed in the forward and backward potential scans, the primary oxidation peak of methanol in PtRu@T/GO was located at nearly −0.28 V, and related peak current density was measured as 876 mA/mg Pt. Also; it is seen that PtRu@T/GO nanocatalysts were 1.82 and 2.32 times more effective compared to the PtRu@GO and Pt/T/GO nanocatalysts, respectively. It can be explained that with the help of T/GO, more active sites can be obtained and give rise to more alcohol oxidation on the surface of the PtRu@T/GO nanocatalysts. This adsorption rate increase can be

Electrode	Ipa (mA/mg metal)	Reference
PtRu@T/GO	876.3 ± 5.2	This work
PtRu/TiO_2-CNF	603	[78]
PtRu/CNF	186	[79]
PtRu/TECNF	516	[80]
TiO_2-PtRu/C	324	[81]
*PtRu/C_{com}	76	[82]

Table 1. Comparison of electrocatalytic activity of different electrode surfaces in 0.5 M CH_3OH in 0.5 M KOH at a scan rate of 50 $mV{\cdot}s^{-1}$. *PtRu/C_{com}: The commercial catalyst.

explained by ascending the active surface area by the aid of T/GO support. Besides, the use of T/GO support in the prepared catalyst prohibits the electrocatalytic reduction in the methanol oxidation reaction and PtRu@T/GO has higher catalytic activity as compared to PtRu@GO, and Pt/T/GO, as shown in Fig. 4a. After obtaining one of the highest currents with the aid of PtRu@T/GO, chronoamperometry (CA) was used for long-term stability tests to compare currents between 1st, 50th, 100th, 200th, 500th and 1000th cycles. It was shown that monodisperse PtRu@T/GO nanocatalysts have better catalytic stability and durability compared to the other prepared ones even after 1000 cycles as shown in Fig. S4. As shown in this Fig. S4, the decreasing of the MOR current in PtRu@GO and Pt@T/GO electrodes is much more compared to the one of PtRu@T/GO electrode. The typical CA curves were recorded on PtRu@GO, Pt@T/GO and PtRu@T/GO for MOR are given in Fig. 4b in an electrolyte solution containing methanol (0.5 M), potassium hydroxide (0.5 M) at -0.28 V for 3600 s. The PtRu@T/GO electrode's current was found to be higher than the other time intervals after 3600 s. The electrodes of PtRu@GO and Pt@T/GO showed a rapid current decay in measurement time compared to the PtRu@T/GO. These findings indicated that the monodisperse PtRu@T/GO electrode shows higher catalytic activity and durability compared to the Pt@T/GO and PtRu@GO electrodes. The electrochemical activities of graphene and graphene oxide supported catalysts used in the literature during methanol oxidation are given in Table 1. In the monometallic case, the oxidation of the platinum decreased because of some poisons like CO, and notably prevented the reaction of methanol oxidation. In PtRu cases, it was thought that ruthenium could react with water, and formed Ru-OH and, strongly bound with CO on Pt, so the PtRu@T/GO and PtRu@GO electrodes had higher catalytic activity and stability for methanol oxidation than Pt@T/GO electrode. Last, but not least, it can also be explained that with the help of T/GO, more active sites were obtained and gave rise to more alcohol oxidation reactions on the surface of the PtRu@T/GO nanomaterials. The electrochemical performance of Pt@T/GO, PtRu@GO, PtRu@T/GO and PtRu and the effects of Pt and Ru contents in the composite on the electrochemical performance in 0.5 M KOH nitrogen saturated solution containing 0.5 M CH_3OH were examined in detail in Tables S1 and S2. As shown in these tables, PtRu@T/GO is the best catalyst compared to the others and 1:1 ratio of Pt and Ru are the optimum ratio for these prepared nanocatalysts.

Conclusions

The current work describes for the controlled synthesis of thiourea functionalized graphene oxide-based PtRu nanocatalysts (PtRu@T/GO) with a series of ultrasonication methods and promises a new catalyst for use in methanol oxidation reactions. Synthesized thiourea (T) based GO (T/GO) was characterized by several morphological techniques and applied as very effective catalysts for the methanol oxidation reactions with the help of the stabilization of T/GO. The method used in this study does not require any expensive systems to prepare natural and environmentally friendly catalysts. PtRu@T/GO indicated an 11-times higher mass activity than PtRu/C_{com}, and a 4-times greater than PtRu/CNF. T/GO is the promising support for the PtRu nanocatalysts for the DMFCs and MOR. The long-term stability of the modified electrode with PtRu@T/GO was also performed with the help of CA and it was found that the activity of PtRu@T/GO was higher than the other prepared ones even after 3600 s. The electrodes of modified with PtRu@GO and Pt@T/GO showed a rapid current decay in measurement time compared to the electrode modified with PtRu@T/GO. Besides, it has been observed that even after 1000 cycles, 97.3% of the initial performance was maintained. These findings indicated that the monodisperse modified PtRu@T/GO electrode shows higher catalytic activity and durability compared to the modified Pt@T/GO and PtRu@GO electrodes. PtRu@T/GO nanocatalysts exhibited a highly recyclable, highly efficient and environmentally friendly for methanol oxidation.

Received: 8 January 2020; Accepted: 24 April 2020;
Published online: 08 May 2020

References

1. Li, J. *et al.* NiSn bimetallic nanoparticles as stable electrocatalysts for methanol oxidation reaction. *Appl. Catal. B Environ.* **234**, 10–18 (2018).
2. Li, C. *et al.* Emerging Pt-based electrocatalysts with highly open nanoarchitectures for boosting oxygen reduction reaction. *Nano Today* **21**, 91–105 (2018).
3. Li, C. *et al.* Electrochemical Deposition: An Advanced Approach for Templated Synthesis of Nanoporous Metal Architectures. *Acc. Chem. Res.* **51**, 1764–1773 (2018).
4. Ataee-Esfahani, H. *et al.* Mesoporous Metallic Cells: Design of Uniformly Sized Hollow Mesoporous Pt-Ru Particles with Tunable Shell Thicknesses. *Small* **9**, 1047–1051 (2013).
5. Li, C. *et al.* Pore-tuning to boost the electrocatalytic activity of polymeric micelle-templated mesoporous Pd nanoparticles. *Chem. Sci.* **10**, 4054–4061 (2019).

6. Ataee-Esfahani, H., Wang, L. & Yamauchi, Y. Block copolymer assisted synthesis of bimetallic colloids with Au core and nanodendritic Pt shell. *Chem. Commun.* **46**, 3684 (2010).
7. Gu, B. *et al*. Effects of the promotion with bismuth and lead on direct synthesis of light olefins from syngas over carbon nanotube supported iron catalysts. *Appl. Catal. B Environ* **234**, 153–166 (2018).
8. Tesfu-Zeru, T., Sakthivel, M. & Drillet, J.-F. Investigation of mesoporous carbon hollow spheres as catalyst support in DMFC cathode. *Appl. Catal. B Environ* **204**, 173–184 (2017).
9. Long, G. *et al*. Pt/CN-doped electrocatalysts: Superior electrocatalytic activity for methanol oxidation reaction and mechanistic insight into interfacial enhancement. *Appl. Catal. B Environ* **203**, 541–548 (2017).
10. Abdel Hameed, R. M. & El-Sherif, R. M. Microwave irradiated nickel nanoparticles on Vulcan XC-72R carbon black for methanol oxidation reaction in KOH solution. *Appl. Catal. B Environ* **162**, 217–226 (2015).
11. Ali, I., AlGhamdi, K. & Al-Wadaani, F. T. Advances in iridium nano catalyst preparation, characterization and applications. *J. Mol. Liq.* **280**, 274–284 (2019).
12. Burakova, E. A. *et al*. Novel and economic method of carbon nanotubes synthesis on a nickel magnesium oxide catalyst using microwave radiation. *J. Mol. Liq.* **253**, 340–346 (2018).
13. Karimi-Maleh, H., Ganjali, M. R., Norouzi, P. & Bananezhad, A. Amplified nanostructure electrochemical sensor for simultaneous determination of captopril, acetaminophen, tyrosine and hydrochlorothiazide. *Mater. Sci. Eng. C* **73**, 472–477 (2017).
14. Karimi-Maleh, H. *et al*. Simultaneous determination of 6-mercaptopruine, 6-thioguanine and dasatinib as three important anticancer drugs using nanostructure voltammetric sensor employing Pt/MWCNTs and 1-butyl-3-methylimidazolium hexafluoro phosphate. *Biosens. Bioelectron.* **86**, 879–884 (2016).
15. Najafi, M., Khalilzadeh, M. A. & Karimi-Maleh, H. A new strategy for determination of bisphenol A in the presence of Sudan I using a ZnO/CNTs/ionic liquid paste electrode in food samples. *Food Chem.* **158**, 125–131 (2014).
16. Qi, J., Benipal, N., Liang, C. & Li, W. PdAg/CNT catalyzed alcohol oxidation reaction for high-performance anion exchange membrane direct alcohol fuel cell (alcohol = methanol, ethanol, ethylene glycol and glycerol). *Appl. Catal. B Environ* **199**, 494–503 (2016).
17. Calderón, J., Calvillo, L., Lázaro, M., Rodríguez, J. & Pastor, E. Effect of the Dendrimer Generation Used in the Synthesis of Pt-Ru Nanoparticles Supported on Carbon Nanofibers on the Catalytic Activity towards Methanol Oxidation. *Energies* **10**, 159 (2017).
18. Zhang, J.-M. *et al*. A strategy in deep eutectic solvents for carbon nanotube-supported PtCo nanocatalysts with enhanced performance toward methanol electrooxidation. *Int. J. Hydrogen Energy* **42**, 26744–26751 (2017).
19. Kim, Y. *et al*. The Role of Ruthenium on Carbon-Supported PtRu Catalysts for Electrocatalytic Glycerol Oxidation under Acidic Conditions. *ChemCatChem* **9**, 1683–1690 (2017).
20. Nie, Q. *et al*. Sensitivity enhanced, stability improved ethanol gas sensor based on multi-wall carbon nanotubes functionalized with Pt-Pd nanoparticles. *Sensors Actuators B Chem.* **270**, 140–148 (2018).
21. Daşdelen, Z., Yıldız, Y., Eriş, S. & Şen, F. Enhanced electrocatalytic activity and durability of Pt nanoparticles decorated on GO-PVP hybride material for methanol oxidation reaction. *Appl. Catal. B Environ*., https://doi.org/10.1016/j.apcatb.2017.08.014 (2017).
22. Eris, S., Daşdelen, Z. & Sen, F. Enhanced electrocatalytic activity and stability of monodisperse Pt nanocomposites for direct methanol fuel cells. *J. Colloid Interface Sci.* **513**, 767–773 (2018).
23. Nakashima, N. & Fujigaya, T. Carbon Nanotube-Based Fuel Cell Catalysts-Comparison with Carbon Black. In 1–28 (Springer, Cham), https://doi.org/10.1007/978-3-319-92917-0_1 (2019).
24. Yoo, E. *et al*. Enhanced Electrocatalytic Activity of Pt Subnanoclusters on Graphene Nanosheet Surface. *Nano Lett.* **9**, 2255–2259 (2009).
25. Yoo, E. *et al*. Sub-nano-Pt cluster supported on graphene nanosheets for CO tolerant catalysts in polymer electrolyte fuel cells. *J. Power Sources* **196**, 110–115 (2011).
26. Siburian, R., Kondo, T. & Nakamura, J. Size Control to a Sub-Nanometer Scale in Platinum Catalysts on Graphene. *J. Phys. Chem. C* **117**, 3635–3645 (2013).
27. Bijad, M., Karimi-Maleh, H. & Khalilzadeh, M. A. Application of ZnO/CNTs Nanocomposite Ionic Liquid Paste Electrode as a Sensitive Voltammetric Sensor for Determination of Ascorbic Acid in Food Samples. *Food Anal. Methods* **6**, 1639–1647 (2013).
28. Elyasi, M., Khalilzadeh, M. A. & Karimi-Maleh, H. High sensitive voltammetric sensor based on Pt/CNTs nanocomposite modified ionic liquid carbon paste electrode for determination of Sudan I in food samples. *Food Chem.* **141**, 4311–4317 (2013).
29. Karimi-Maleh, H. *et al*. A high sensitive biosensor based on FePt/CNTs nanocomposite/N-(4-hydroxyphenyl)-3,5-dinitrobenzamide modified carbon paste electrode for simultaneous determination of glutathione and piroxicam. *Biosens. Bioelectron.* **60**, 1–7 (2014).
30. Wang, Q. Enhanced Activity for Methanol Electro-oxidation on PtRu/C Catalyst by Reduction Treatment. *Int. J. Electrochem. Sci.* **12**, 6211–6220 (2017).
31. Elinson, M. N. *et al*. The first example of the cascade assembly of a spirocyclopropane structure: direct transformation of benzylidenemalononitriles and N,N′-dialkylbarbituric acids into substituted 2-aryl-4,6,8-trioxo-5,7-diazaspiro[2.5]octane-1,1-dicarbonitriles. *Tetrahedron Lett.* **51**, 428–431 (2010).
32. Burhan, H., Ay, H., Kuyuldar, E. & Sen, F. Monodisperse Pt-Co/GO anodes with varying Pt: Co ratios as highly active and stable electrocatalysts for methanol electrooxidation reaction. *Sci. Rep.* **10**, 6114 (2020).
33. Kaplan, D., Burstein, L., Popov, I. & Peled, E. The Effect of Different Pt:Ru Surface Composition on Methanol-Oxidation Activity of Carbon-Supported PtRu/IrNi Catalysts. *J. Electrochem. Soc.* **163**, F1004–F1010 (2016).
34. Li, M., Zheng, H., Han, G., Xiao, Y. & Li, Y. Facile synthesis of binary PtRu nanoflowers for advanced electrocatalysts toward methanol oxidation. *Catal. Commun.* **92**, 95–99 (2017).
35. Xu, H. *et al*. Facile synthesis of Pd-Ru-P ternary nanoparticle networks with enhanced electrocatalytic performance for methanol oxidation. *Int. J. Hydrogen Energy* **42**, 11229–11238 (2017).
36. Wang, L., Mao, H., Zhou, X., Xu, Q. & Li, Q. The Impregnating Reduction Method for Synthesis of Pt–Ru Nanoparticles and Its Catalytic Performance for Methanol Electro-oxidation. *J. Fuel Cell Sci. Technol* **12**, 041001 (2015).
37. Zhao, Y., Fan, L., Ren, J. & Hong, B. Electrodeposition of Pt–Ru and Pt–Ru–Ni nanoclusters on multi-walled carbon nanotubes for direct methanol fuel cell. *Int. J. Hydrogen Energy* **39**, 4544–4557 (2014).
38. Wu, B. *et al*. Functionalization of Carbon Nanotubes by an Ionic-Liquid Polymer: Dispersion of Pt and PtRu Nanoparticles on Carbon Nanotubes and Their Electrocatalytic Oxidation of Methanol. *Angew. Chemie Int. Ed.* **48**, 4751–4754 (2009).
39. Yousaf, A. Bin *et al*. Enhanced and durable electrocatalytic performance of thin layer PtRu bimetallic alloys on Pd-nanocubes for methanol oxidation reactions. *Catal. Sci. Technol.* **7**, 3283–3290 (2017).
40. Davies, D., Golunski, S., Johnston, P., Lalev, G. & Taylor, S. H. Dominant Effect of Support Wettability on the Reaction Pathway for Catalytic Wet Air Oxidation over Pt and Ru Nanoparticle Catalysts. *ACS Catal.* **8**, 2730–2734 (2018).
41. Huang, L. *et al*. Shape-Control of Pt–Ru Nanocrystals: Tuning Surface Structure for Enhanced Electrocatalytic Methanol Oxidation. *J. Am. Chem. Soc.* **140**, 1142–1147 (2018).
42. Kuyuldar, E. *et al*. Enhanced Electrocatalytic Activity and Durability of PtRu Nanoparticles Decorated on rGO Material for Ethanol Oxidation Reaction. In *Graphene Functionalization Strategies* 389–398, https://doi.org/10.1007/978-981-32-9057-0_16 (2019).
43. Schoekel, A. *et al*. Quantitative study of ruthenium cross-over in direct methanol fuel cells during early operation hours. *J. Power Sources* **301**, 210–218 (2016).
44. Darowicki, K. & Gawel, L. Impedance Measurement and Selection of Electrochemical Equivalent Circuit of a Working PEM Fuel Cell Cathode. *Electrocatalysis* **8**, 235–244 (2017).

45. Ensafi, A. A., Jafari-Asl, M. & Rezaei, B. A new strategy for the synthesis of 3-D Pt nanoparticles on reduced graphene oxide through surface functionalization, Application for methanol oxidation and oxygen reduction. *Electrochim. Acta* **130**, 397–405 (2014).
46. Marquardt, D. *et al*. Hybrid materials of platinum nanoparticles and thiol-functionalized graphene derivatives. *Carbon N. Y* **66**, 285–294 (2014).
47. Sharma, S. *et al*. Rapid Microwave Synthesis of CO Tolerant Reduced Graphene Oxide-Supported Platinum Electrocatalysts for Oxidation of Methanol. *J. Phys. Chem. C* **114**, 19459–19466 (2010).
48. Shang, N., Papakonstantinou, P., Wang, P. & Silva, S. R. P. Platinum Integrated Graphene for Methanol Fuel Cells. *J. Phys. Chem. C* **114**, 15837–15841 (2010).
49. Zhang, L., Gao, A., Liu, Y., Wang, Y. & Ma, J. PtRu nanoparticles dispersed on nitrogen-doped carbon nanohorns as an efficient electrocatalyst for methanol oxidation reaction. *Electrochim. Acta* **132**, 416–422 (2014).
50. Cao, L. *et al*. Novel Nanocomposite Pt/RuO2·x H2O/Carbon Nanotube Catalysts for Direct Methanol Fuel Cells. *Angew. Chemie Int. Ed* **45**, 5315–5319 (2006).
51. Zhang, Q. *et al*. Carbon nitride simultaneously boosted a PtRu electrocatalyst's stability and electrocatalytic activity toward concentrated methanol. *Chem. Commun.* **54**, 9282–9285 (2018).
52. Xu, G. A comparative study on electrocatalytic performance of PtAu/C and PtRu/C nanoparticles for methanol oxidation reaction. *Ionics (Kiel)* **24**, 3915–3921 (2018).
53. Wu, B. *et al*. PtRu nanoparticles supported on p-phenylenediamine-functionalized multiwalled carbon nanotubes: enhanced activity and stability for methanol oxidation. *Ionics (Kiel)* **25**, 181–189 (2019).
54. Xu, H. *et al*. Eco-friendly and facile synthesis of novel bayberry-like PtRu alloy as efficient catalysts for ethylene glycol electrooxidation. *Int. J. Hydrogen Energy* **42**, 20720–20728 (2017).
55. Alcaide, F. *et al*. Effect of the solvent in the catalyst ink preparation on the properties and performance of unsupported PtRu catalyst layers in direct methanol fuel cells. *Electrochim. Acta* **231**, 529–538 (2017).
56. Hu, Z., Qin, S., Li, Z., Zhu, Y. & Liu, W. Two-dimensional PtRu Nanoclusters Carbon Based Electrocatalysts for Methanol Oxidation. *J. Wuhan Univ. Technol. Sci. Ed* **33**, 537–540 (2018).
57. Mohanraj, J. *et al*. Facile synthesis of paper based graphene electrodes for point of care devices: A double stranded DNA (dsDNA) biosensor. *J. Colloid Interface Sci.* **566**, 463–472 (2020).
58. Karimi-Maleh, H. *et al*. The role of magnetite/graphene oxide nano-composite as a high-efficiency adsorbent for removal of phenazopyridine residues from water samples, an experimental/theoretical investigation. *J. Mol. Liq.* **298**, 112040 (2020).
59. Karimi-Maleh, H. & Arotiba, O. A. Simultaneous determination of cholesterol, ascorbic acid and uric acid as three essential biological compounds at a carbon paste electrode modified with copper oxide decorated reduced graphene oxide nanocomposite and ionic liquid. *J. Colloid Interface Sci.* **560**, 208–212 (2020).
60. Tahernejad-Javazmi, F., Shabani-Nooshabadi, M. & Karimi-Maleh, H. 3D reduced graphene oxide/FeNi3-ionic liquid nanocomposite modified sensor; an electrical synergic effect for development of tert-butylhydroquinone and folic acid sensor. *Compos. Part B Eng.* **172**, 666–670 (2019).
61. Khodadadi, A. *et al*. A new epirubicin biosensor based on amplifying DNA interactions with polypyrrole and nitrogen-doped reduced graphene: Experimental and docking theoretical investigations. *Sensors Actuators B Chem.* **284**, 568–574 (2019).
62. Sen, B., Şavk, A. & Sen, F. Highly efficient monodisperse Pt nanoparticles confined in the carbon black hybrid material for hydrogen liberation. *J. Colloid Interface Sci.* **520**, 112–118 (2018).
63. Şen, B. *et al*. Bimetallic PdRu/graphene oxide based Catalysts for one-pot three-component synthesis of 2-amino-4H-chromene derivatives. *Nano-Structures & Nano-Objects* **12**, 33–40 (2017).
64. Şen, B. *et al*. A novel thiocarbamide functionalized graphene oxide supported bimetallic monodisperse Rh-Pt nanoparticles (RhPt/TC@GO NPs) for Knoevenagel condensation of aryl aldehydes together with malononitrile. *Appl. Catal. B Environ.* **225**, 148–153 (2018).
65. Eris, S., Daşdelen, Z. & Sen, F. Investigation of electrocatalytic activity and stability of Pt@f-VC catalyst prepared by *in-situ* synthesis for Methanol electrooxidation. *Int. J. Hydrogen Energy*, https://doi.org/10.1016/j.ijhydene.2017.11.063 (2018)
66. Eris, S., Daşdelen, Z., Yıldız, Y. & Sen, F. Nanostructured Polyaniline-rGO decorated platinum catalyst with enhanced activity and durability for Methanol oxidation. *Int. J. Hydrogen Energy*, https://doi.org/10.1016/j.ijhydene.2017.11.051 (2018)
67. Yıldız, Y. *et al*. Different ligand based monodispersed Pt nanoparticles decorated with rGO as highly active and reusable catalysts for the methanol oxidation. *Int. J. Hydrogen Energy*, https://doi.org/10.1016/j.ijhydene.2017.03.230 (2017)
68. Planeix, J. M. *et al*. Application of Carbon Nanotubes as Supports in Heterogeneous Catalysis. *J. Am. Chem. Soc.* **116**, 7935–7936 (1994).
69. Huang, H. *et al*. Worm-Shape Pt Nanocrystals Grown on Nitrogen-Doped Low-Defect Graphene Sheets: Highly Efficient Electrocatalysts for Methanol Oxidation Reaction. *Small* **13**, 1603013 (2017).
70. Sen, B., Kuzu, S., Demir, E., Onal Okyay, T. & Sen, F. Hydrogen liberation from the dehydrocoupling of dimethylamine–borane at room temperature by using novel and highly monodispersed RuPtNi nanocatalysts decorated with graphene oxide. *Int. J. Hydrogen Energy*, https://doi.org/10.1016/j.ijhydene.2017.04.213 (2017)
71. Demirci, T. *et al*. One-pot synthesis of Hantzsch dihydropyridines using a highly efficient and stable PdRuNi@GO catalyst. *RSC Adv.* **6**, 76948–76956 (2016).
72. Pamuk, H., Aday, B., Şen, F. & Kaya, M. Pt NPs@GO as a highly efficient and reusable catalyst for one-pot synthesis of acridinedione derivatives. *RSC Adv.* **5**, 49295–49300 (2015).
73. Çelik, B. *et al*. Monodisperse Pt(0)/DPA@GO nanoparticles as highly active catalysts for alcohol oxidation and dehydrogenation of DMAB. *Int. J. Hydrogen Energy* **41**, 5661–5669 (2016).
74. Yıldız, Y., Pamuk, H., Karatepe, Ö., Dasdelen, Z. & Sen, F. Carbon black hybrid material furnished monodisperse platinum nanoparticles as highly efficient and reusable electrocatalysts for formic acid electro-oxidation. *RSC Adv.* **6**, 32858–32862 (2016).
75. Ozturk, Z., Sen, F., Sen, S. & Gokagac, G. The preparation and characterization of nano-sized Pt–Pd/C catalysts and comparison of their superior catalytic activities for methanol and ethanol oxidation. *J. Mater. Sci.* **47**, 8134–8144 (2012).
76. Şen, S., Şen, F. & Gökağaç, G. Preparation and characterization of nano-sized Pt-Ru/C catalysts and their superior catalytic activities for methanol and ethanol oxidation. *Phys. Chem. Chem. Phys*., https://doi.org/10.1039/c1cp20064j (2011)
77. Yıldız, Y., Erken, E., Pamuk, H., Sert, H. & Şen, F. Monodisperse Pt Nanoparticles Assembled on Reduced Graphene Oxide: Highly Efficient and Reusable Catalyst for Methanol Oxidation and Dehydrocoupling of Dimethylamine-Borane (DMAB). *J. Nanosci. Nanotechnol.* **16**, 5951–5958 (2016).
78. Abdullah, N., Kamarudin, S. K., Shyuan, L. K. & Karim, N. A. Synthesis and optimization of PtRu/TiO 2 -CNF anodic catalyst for direct methanol fuel cell. *Int. J. Hydrogen Energy* **44**, 30543–30552 (2018).
79. Abdullah, N., Kamarudin, S. K. & Shyuan, L. K. Novel Anodic Catalyst Support for Direct Methanol Fuel Cell: Characterizations and Single-Cell Performances. *Nanoscale Res. Lett.* **13**, 90 (2018).
80. Ito, Y., Takeuchi, T., Tsujiguchi, T., Abdelkareem, M. A. & Nakagawa, N. Ultrahigh methanol electro-oxidation activity of PtRu nanoparticles prepared on TiO_2-embedded carbon nanofiber support. *J. Power Sources* **242**, 280–288 (2013).
81. Kolla, P. & Smirnova, A. Methanol oxidation on hybrid catalysts: PtRu/C nanostructures promoted with cerium and titanium oxides. *Int. J. Hydrogen Energy* **38**, 15152–15159 (2013).
82. Tsukagoshi, Y., Ishitobi, H. & Nakagawa, N. Improved performance of direct methanol fuel cells with the porous catalyst layer using highly-active nanofiber catalyst. *Carbon Resour. Convers* **1**, 61–72 (2018).

Acknowledgements
The authors would like to thank Gaziantep University for funding (FEF.YLT.18.14). The author(s) declare no competing interests.

Author contributions
A.I. and F.S. organized all experiments and wrote the manuscript. E.K., S.S.P., H.B. and S.D.M. performed all experiments and characterizations. They have also drawn the figures.

Competing interests
The authors declare no competing interests.

Additional information
Supplementary information is available for this paper at https://doi.org/10.1038/s41598-020-64885-6.

Correspondence and requests for materials should be addressed to F.S.

Reprints and permissions information is available at www.nature.com/reprints.

Publisher's note Springer Nature remains neutral with regard to jurisdictional claims in published maps and institutional affiliations.